Expanded View Figures

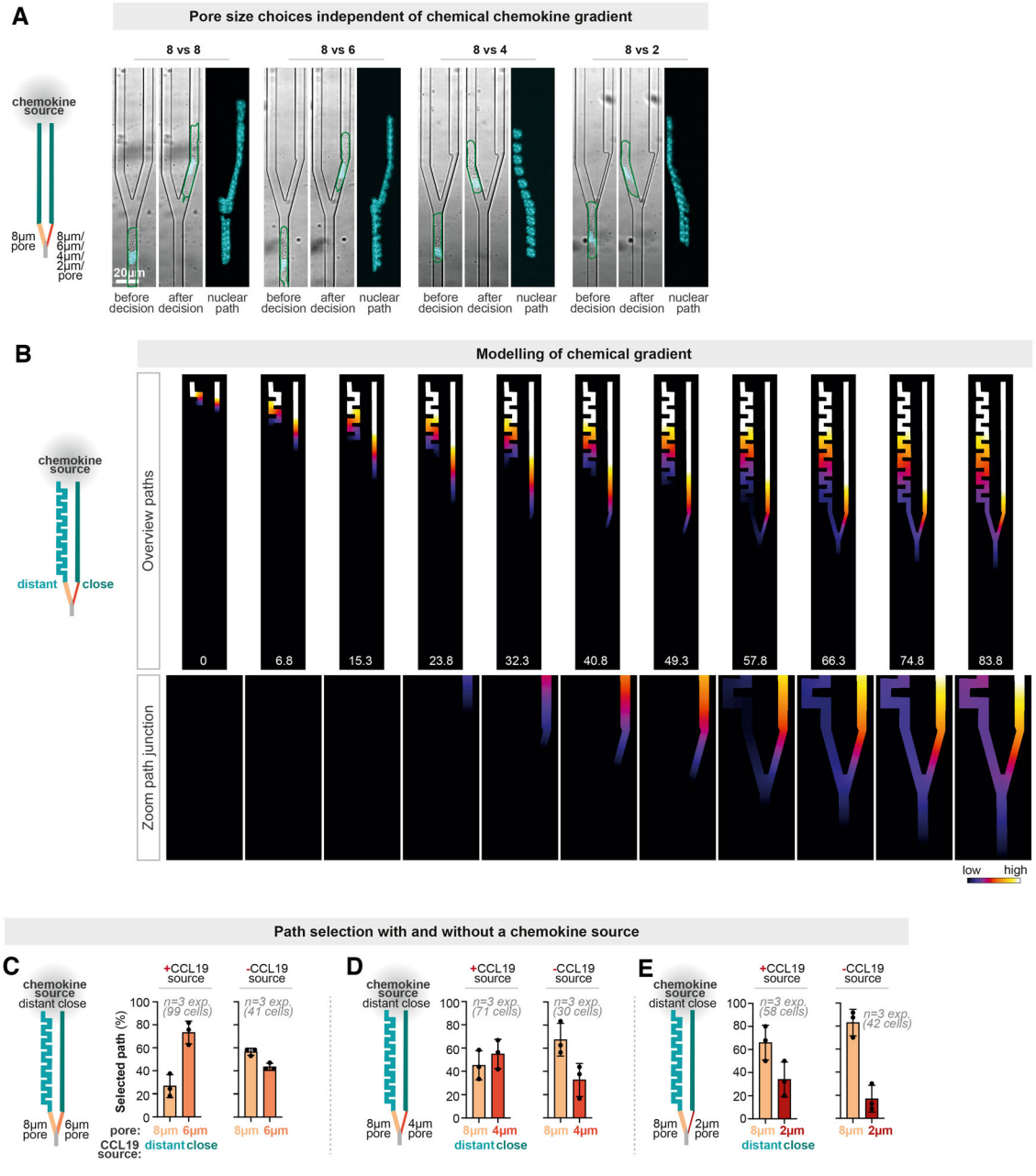

Figure EV1.

Figure EV1. Novel reductionistic assays to characterize cellular path choices in competing chemokine and pore size gradients.

A Representative bone marrow-derived DCs (BMDC) migrating in microchannels with two-way path junctions with different pore sizes (8 vs. 8; 8 vs. 6; 8 vs. 4; or 8 vs. 2 μm) but an equally long and symmetric path towards the chemokine source. The cell shape is outlined in green and the nucleus is visualized by Hoechst (cyan). See Fig 2A for quantification.

B Time-dependent simulation of CCL19 diffusion at a two-way path junction (with a diffusion constant of 1.3e-10 m^2/s), at one path is closer to the source of the chemokine than the alternative path, which follows a snake-like pattern and thus is more distant to the chemokine source. Time in seconds.

C Quantification of cellular path decisions in microenvironments of competing chemokine and pore size gradients (as shown in Fig 2C) with and without chemokines source. $N = 3$ replicates (99 cells +CCL19; 41 cells without CCL19). Note that the comparative dataset of cells with CCL19 is the same data as in main Fig 2F. Data are Mean ± SD.

D Quantification of cellular path decisions in microenvironments of competing chemokine and pore size gradients (as shown in Fig 2D) with and without chemokines source. $N = 3$ replicates (71 cells +CCL19; 30 cells without CCL19). Note that the comparative dataset of cells with CCL19 is the same data as in main Fig 2G. Data are Mean ± SD.

E Quantification of cellular path decisions in microenvironments of competing chemokine and pore size gradients (as shown in Fig 2E) with and without chemokines source. $N = 3$ replicates (58 cells +CCL19; 42 cells without CCL19). Note that the comparative dataset of cells with CCL19 is the same data as in main Fig 2H. Data are Mean ± SD.

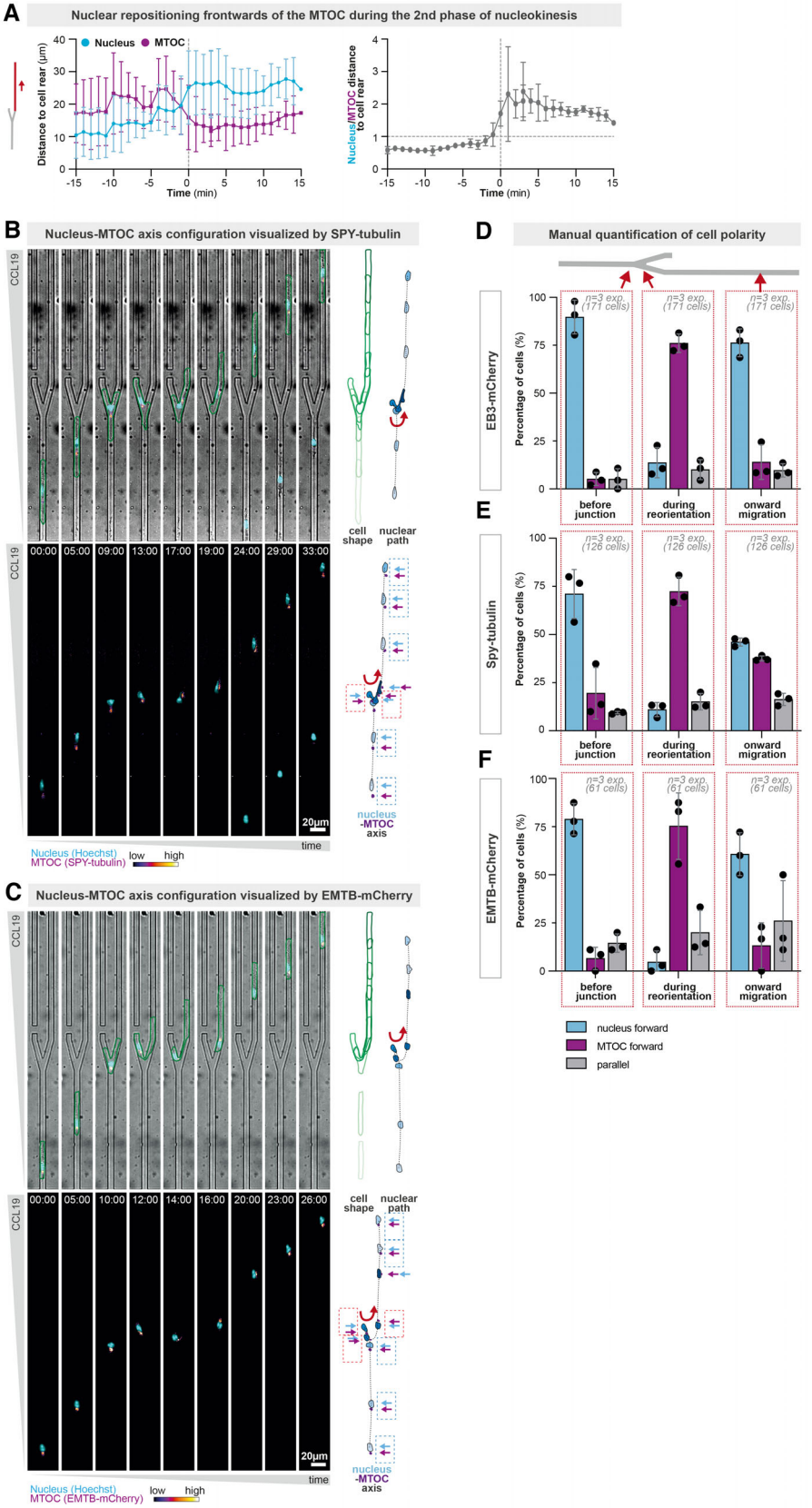

Figure EV2. Quantification of re-orientations in the configuration of the nucleus-MTOC axis during amoeboid nucleokinesis.

A Quantification of the distance of the nucleus and MTOC to the cell rear during the second phase of nucleokinesis, showing that the nucleus moves intracellularly into the front of the MTOC (left panel); the right panel shows the same data but plotting the ratios of nucleus and MTOC distances to the cell rear, highlighting that the nucleus increases its distance to the cell rear during the second phase of nucleokinesis. Data are mean ± SD. $N = 5$ replicates, 8 cells.

B Representative Hoxb8-derived dendritic cell (DC) approaching a path decision with equal pores sizes but one blocked path, frequently causing nucleokinesis from the blocked to the open path. The DC is stained with SPY-tubulin, which also visualizes the microtubule-organizing center (MTOC; in pink). The nucleus is visualized by Hoechst (cyan) and the cell shape is outlined in green. Projections of cellular (green), MTOC (pink) and nuclear (blue) paths are shown on the right. The configuration of the nucleus-MTOC axis is highlighted by dashed boxes (blue = nucleus forward; red = MTOC forward). Time in min:s.

C As in (B), but using DCs that stably encode EMTB-mCherry, which visualizes the microtubule-organizing center.

D Manual quantification of the nucleus-MTOC axis configuration in EB3-mCherry expressing Hoxb8-derived dendritic cells before, during, and after nucleokinesis. The nucleus-MTOC axis configuration was assessed at the channel regions indicated by the red arrows. $N = 3$ replicates, 171 cells. Data are mean ± SD.

E Manual quantification of the nucleus-MTOC axis configuration in SPY-tubulin stained Hoxb8-derived dendritic cells before, during, and after nucleokinesis. The nucleus-MTOC axis configuration was assessed at the channel regions indicated by the red arrows. $N = 3$ replicates, 126 cells. Data are mean ± SD.

F Manual quantification of the nucleus-MTOC axis configuration in EMTB-mCherry expressing Hoxb8-derived dendritic cells before, during, and after nucleokinesis. The nucleus-MTOC axis configuration was assessed at the channel regions indicated by the red arrows. $N = 3$ replicates, 61 cells. Data are mean ± SD.

Figure EV3. Amoeboid nucleokinesis remains largely unaffected when microtubules are depolymerized.

A Heatmap of nuclear speed during amoeboid nucleokinesis in the presence of the microtubule inhibitor nocodazole (300 nM) or control (DMSO). The yellow-dotted regions 1 (DMSO) and 2 (Nocodazole) are enlarged to depict the cellular behavior during the initial nucleokinesis event. $N = 3$ replicates, 96 (DMSO) and 38 (Nocodazole) cells.

B Quantification of nuclear speed during amoeboid nucleokinesis upon microtubule inhibition with 300 nM nocodazole (Nocod.): EMTB-mCherry expressing HoxB8-derived DCs, migrating through a path junction with one blocked path. The data show tracked nuclear velocities (visualized by Hoechst) of DCs that reposition their nucleus from the blocked to the open path by nucleokinesis. $N = 3$ replicates, 96 (DMSO) and 38 (Nocodazole), total analyzed events per column (from 1st to last column): 859, 417, 235, 45, 305, 145, 188, 58, 34, 23, 304, 149, 111, 81, 249, 46, 577, 505, 484, 97; mean ± 95CI, Mann–Whitney test.

C As in (A), but in the presence of 10 μM nocodazole. $N = 4$ replicates, 71 (DMSO) and 48 (Nocodazole) cells.

D As in (B), but in the presence of 10 μM nocodazole. $N = 4$ replicates, 71 (DMSO) and 48 (Nocodazole) cells, total analyzed events per column (from 1st to last column): 1140, 671, 426, 292, 263, 231, 297, 180, 997, 768; mean ± 95CI, Mann–Whitney test.

E Heatmap of distance between nucleus and MTOC during amoeboid nucleokinesis in the presence of the microtubule inhibitor nocodazole (300 nM) or control (DMSO). The yellow-dotted regions 1 (DMSO) and 2 (Nocodazole) are enlarged to depict the cellular behavior during the initial nucleokinesis event. $N = 3$ replicates, 96 (DMSO) and 38 (Nocodazole) cells.

F Distances between the MTOC and the nucleus during nucleokinesis in representative EMTB-mCherry expressing Hoxb8-derived dendritic cells in control (DMSO) and microtubule inhibited (300 nM nocodazole) samples. See (E) and (G) for quantification of the distance between MTOC and nucleus during the different phases of nucleokinesis. Some of the categories (MTOC in front in same channel parts) occurred rarely at the channel entrance, preventing representative images.

G Quantification of the distance between nucleus and MTOC during amoeboid nucleokinesis upon microtubule inhibition with 300 nM nocodazole (Nocod.): EMTB-mCherry expressing HoxB8-derived DCs, migrating through a path junction with one blocked path. The data show the distances between the center of the nucleus (visualized by Hoechst) and the center of the MTOC (visualized by EMTB-mCherry) in DCs that reposition their nucleus from the blocked to the open path by nucleokinesis. The red dashed boxes highlight the reduced distance between nucleus and MTOC upon microtubule inhibition, when the MTOC is positioned frontward. $N = 3$ replicates, 96 (DMSO) and 38 (Nocodazole), total analyzed events per column (from 1st to last column): 859, 417, 237, 46, 305, 145, 188, 58, 34, 23, 304, 149, 111, 81, 249, 46, 578, 508, 484, 97; mean ± 95CI; Mann–Whitney test.

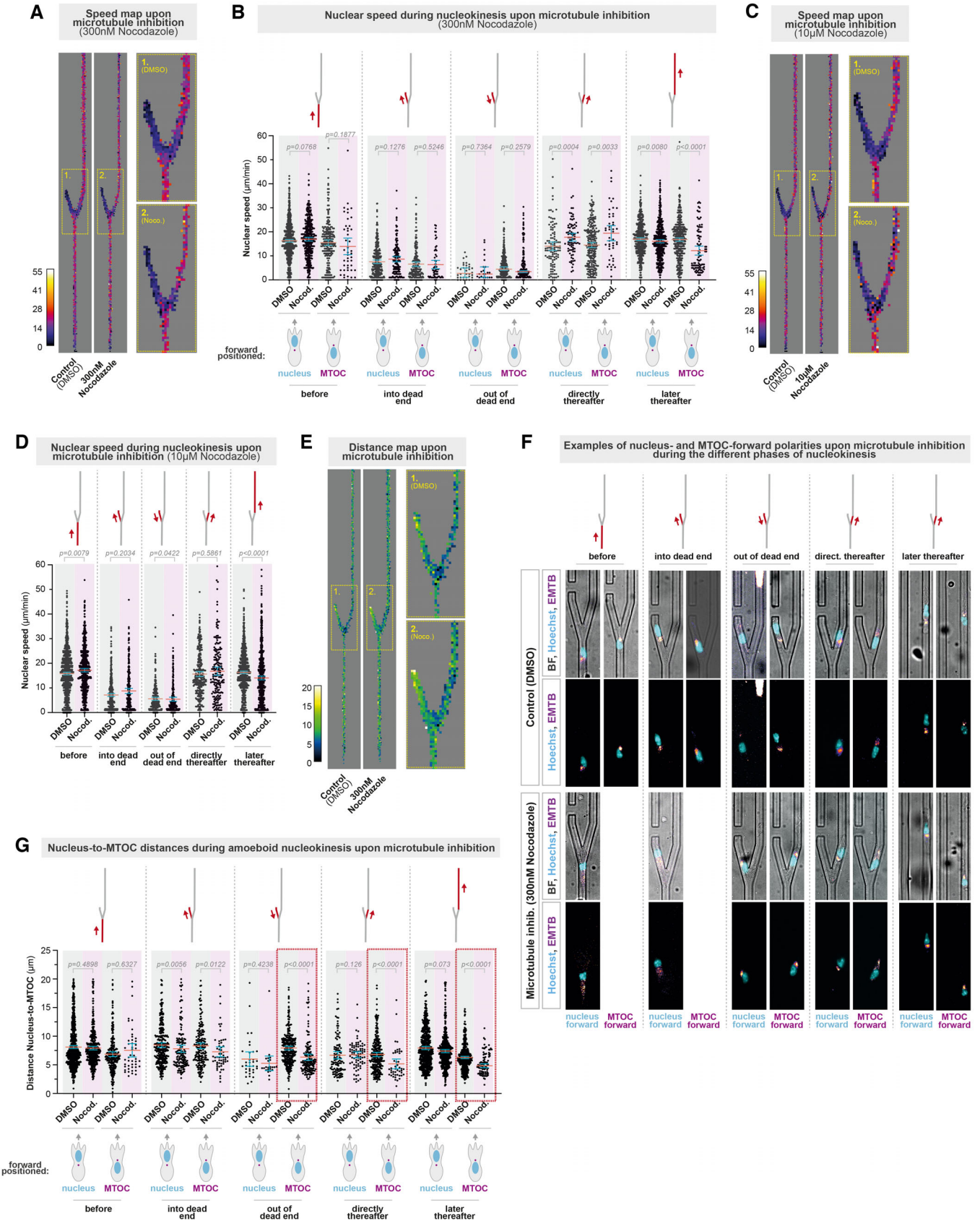
A
Speed map upon microtubule inhibition (300nM Nocodazole)
1. (DMSO)
2. (Noco.)
Control (DMSO)
300nM Nocodazole
B
Nuclear speed during nucleokinesis upon microtubule inhibition (300nM Nocodazole)
Nuclear speed (µm/min)
forward positioned:
nucleus
MTOC
before
into dead end
out of dead end
directly thereafter
later thereafter
C
Speed map upon microtubule inhibition (10µM Nocodazole)
10µM Nocodazole
D
Nuclear speed during nucleokinesis upon microtubule inhibition (10µM Nocodazole)
E
Distance map upon microtubule inhibition
F
Examples of nucleus- and MTOC-forward polarities upon microtubule inhibition during the different phases of nucleokinesis
Control (DMSO)
Microtubule inhib. (300nM Nocodazole)
BF, Hoechst, EMTB
Hoechst, EMTB
direct. thereafter
G
Nucleus-to-MTOC distances during amoeboid nucleokinesis upon microtubule inhibition
Distance Nucleus-to-MTOC (µm)

Figure EV3.

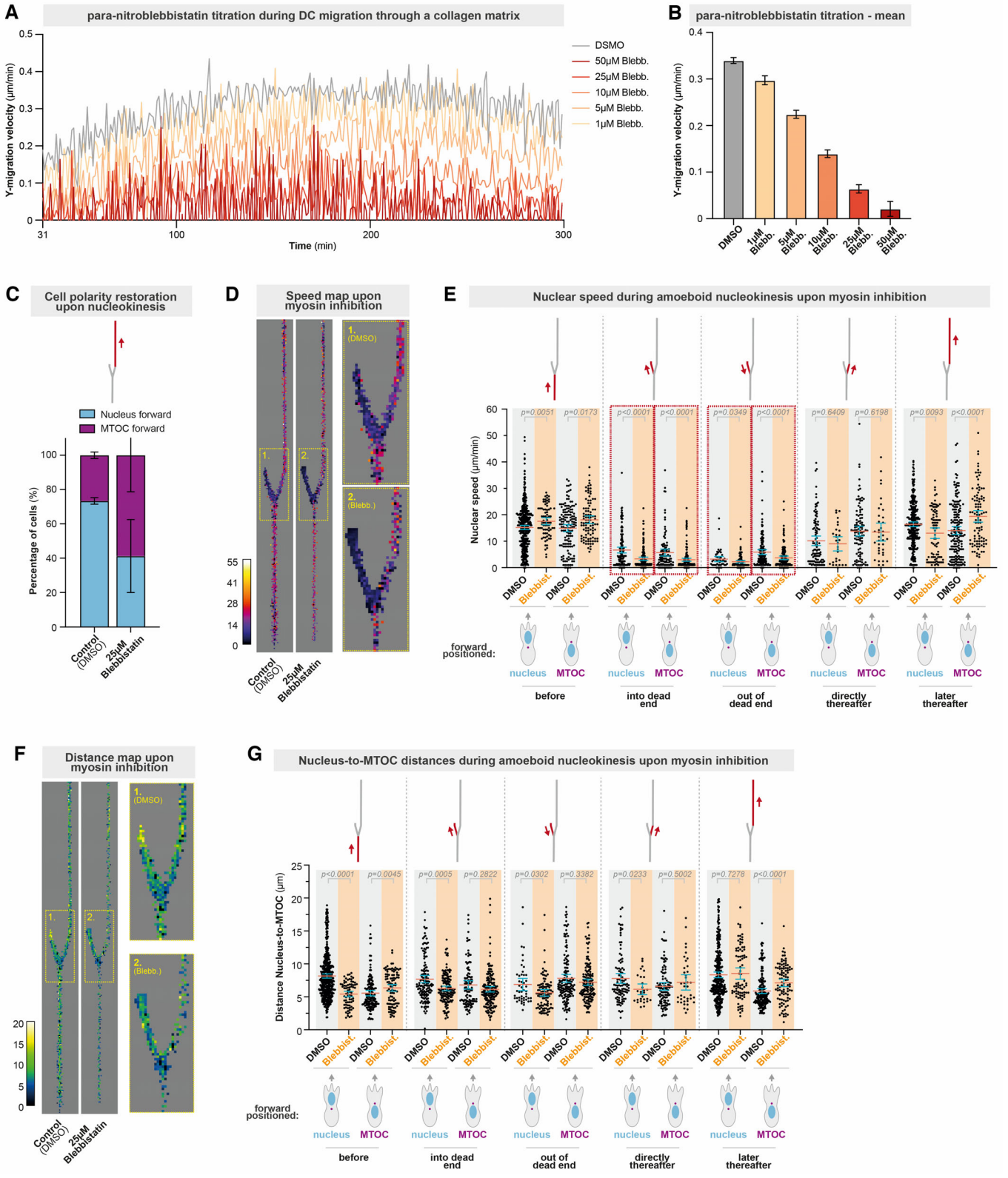

Figure EV4.

Figure EV4. Reduced amoeboid nucleokinesis speed and cell polarity switching upon myosin inhibition.

A Bone marrow-derived dendritic cell migration in three-dimensional (3D) collagen matrices (3.3 mg/ml) along a CCL19 chemokine gradient in the presence of different concentrations of para-nitroblebbistatin (myosin inhibitor) or DMSO (control). $N = 3$ replicates. Data are mean.

B Mean migration velocity between 150 and 250 min of cells shown in (A). $N = 3$ replicates. Data are mean ± 95CI.

C Quantification of the cell polarity after nucleokinesis at the channel exit in the presence of the myosin inhibitor para-nitroblebbistatin (25 μM) or control (DMSO). $N = 4$ replicates, 37 (DMSO) and 13 (para-nitroblebbistatin) cells. Data are mean ± SEM.

D Heatmap of nuclear speed during amoeboid nucleokinesis in the presence of the myosin inhibitor para-nitroblebbistatin (25 μM) or control (DMSO). The yellow-dotted regions 1 (DMSO) and 2 (para-nitroblebbistatin) are enlarged to depict the cellular behavior during the initial nucleokinesis event. $N = 4$ replicates, 37 (DMSO) and 13 (Blebbist.) cells.

E Quantification of nuclear speed during amoeboid nucleokinesis upon myosin inhibition with 25 μM para-nitroblebbistatin (Blebbist.): EB3-mCherry expressing HoxB8-derived DCs, migrating through a path junction with one blocked path. The data show tracked nuclear velocities (visualized by Hoechst) of DCs that reposition their nucleus from the blocked to the open path by nucleokinesis. The red dashed boxes highlight the decelerated nuclear speed upon myosin inhibition during repositioning of the nucleus from the blocked path. $N = 4$ replicates, 37 (DMSO) and 13 (Blebbist.) cells; total analyzed events per column (from 1st to last column): 433, 76, 146, 97, 139, 147, 107, 168, 48, 99, 150, 145, 101, 29, 107, 38, 330, 83, 184, 97; mean ± 95CI, Mann–Whitney test.

F Heatmap of distance between nucleus and MTOC during amoeboid nucleokinesis in the presence of the myosin inhibitor para-nitroblebbistatin (25 μM) or control (DMSO). The yellow-dotted regions 1 (DMSO) and 2 (Blebbist.) are enlarged to depict the cellular behavior during the initial nucleokinesis event. $N = 4$ replicates, 37 (DMSO) and 13 (Blebbist.) cells.

G Quantification of the distance between nucleus and MTOC during amoeboid nucleokinesis upon myosin inhibition with 25 μM para-nitroblebbistatin (Blebbist.): EB3-mCherry expressing HoxB8-derived DCs, migrating through a path junction with one blocked path. The data show the distances between the center of the nucleus (visualized by Hoechst) and the center of the MTOC (visualized by EB3-mCherry) in DCs that reposition their nucleus from the blocked to the open path by nucleokinesis. $N = 4$ replicates, 37 (DMSO) and 13 (Blebbist.) cells, total analyzed events per column (from 1st to last column): 433, 76, 146, 97, 139, 147, 107, 168, 48, 99, 150, 145, 101, 29, 107, 38, 330, 83, 184, 97; mean ± 95CI, Mann–Whitney test.

Figure EV5. Delayed cell polarity switching and amoeboid nucleokinesis upon low-dose actin inhibition.

A Bone marrow-derived dendritic cell migration in three-dimensional (3D) collagen matrices (3.3 mg/ml) along a CCL19 chemokine gradient in the presence of different concentrations of Latrunculin A (actin inhibitor) or DMSO (control). $N = 3$ replicates. Data are mean.

B Mean migration velocity between 150 and 250 min of cells shown in (A). $N = 3$ replicates. Data are mean ± 95CI.

C Heatmap of the nucleus-MTOC axis configuration during amoeboid nucleokinesis in the presence of the actin inhibitor Latrunculin A (50 nM) or control (DMSO). The yellow-dotted regions 1 (DMSO) and 2 (Latrunculin A) are enlarged to depict the cellular behavior during the initial nucleokinesis event, and the yellow-dotted regions 3 (DMSO) and 4 (Latrunculin A) are enlarged to depict the cellular behavior during the later nucleokinesis events to reposition the nucleus to the cellular front. $N = 3$ replicates, 78 (DMSO) and 67 (Latrunculin A) cells.

D Quantification of the cell polarity after nucleokinesis at the channel exit in the presence of the actin inhibitor Latrunculin A (50 nM) or control (DMSO). $N = 3$ replicates, 78 (DMSO) and 66 (Latrunculin A) cells. Data are mean ± SEM.

E Quantification of the duration of nucleokinesis in the presence of the actin inhibitor Latrunculin A (50 nM) or control (DMSO). $N = 3$ replicates, 101 (DMSO) and 93 (Latrunculin A) cells. Data are mean ± SEM.

F Heatmap of nuclear speed during amoeboid nucleokinesis in the presence of the actin inhibitor Latrunculin A (50 nM) or control (DMSO). The yellow-dotted regions 1 (DMSO) and 2 (Latrunculin A) are enlarged to depict the cellular behavior during the initial nucleokinesis event. $N = 3$ replicates, 78 (DMSO) and 67 (Latrunculin A) cells.

G Quantification of nuclear speed during amoeboid nucleokinesis upon actin inhibition with 50 nM Latrunculin A (Latr. A): EB3-mCherry expressing HoxB8-derived DCs, migrating through a path junction with one blocked path. The data show tracked nuclear velocities (visualized by Hoechst) of DCs that reposition their nucleus from the blocked to the open path by nucleokinesis. The red dashed boxes highlight the decelerated nuclear speed upon actin inhibition during repositioning of the nucleus from the blocked path. $N = 3$ replicates, 78 (DMSO) and 67 (Latr. A) cells, total analyzed events per column (from 1st to last column): 684, 444, 206, 413, 210, 204, 113, 147, 50, 48, 184, 217, 155, 119, 127, 209, 700, 434, 201, 465; data are mean ± 95CI, Mann–Whitney test.

H Heatmap of distance between nucleus and MTOC during amoeboid nucleokinesis in the presence of the actin inhibitor Latrunculin A (50 nM) or control (DMSO). The yellow-dotted regions 1 (DMSO) and 2 (Latr. A) are enlarged to depict the cellular behavior during the initial nucleokinesis event. $N = 3$ replicates, 78 (DMSO) and 67 (Latr. A) cells.

I Quantification of the distance between nucleus and MTOC during amoeboid nucleokinesis upon actin inhibition with 50 nM Latrunculin A (Latr. A): EB3-mCherry expressing HoxB8-derived DCs, migrating through a path junction with one blocked path. The data show the distances between the center of the nucleus (visualized by Hoechst) and the center of the MTOC (visualized by EB3-mCherry) in DCs that reposition their nucleus from the blocked to the open path by nucleokinesis. $N = 3$ replicates, 78 (DMSO) and 67 (Latr. A) cells, total analyzed events per column (from 1st to last column): 684, 444, 206, 413, 210, 204, 113, 147, 50, 48, 184, 217, 155, 119, 127, 209, 700, 434, 201, 465; data are mean ± 95CI, Mann-Whitney test.

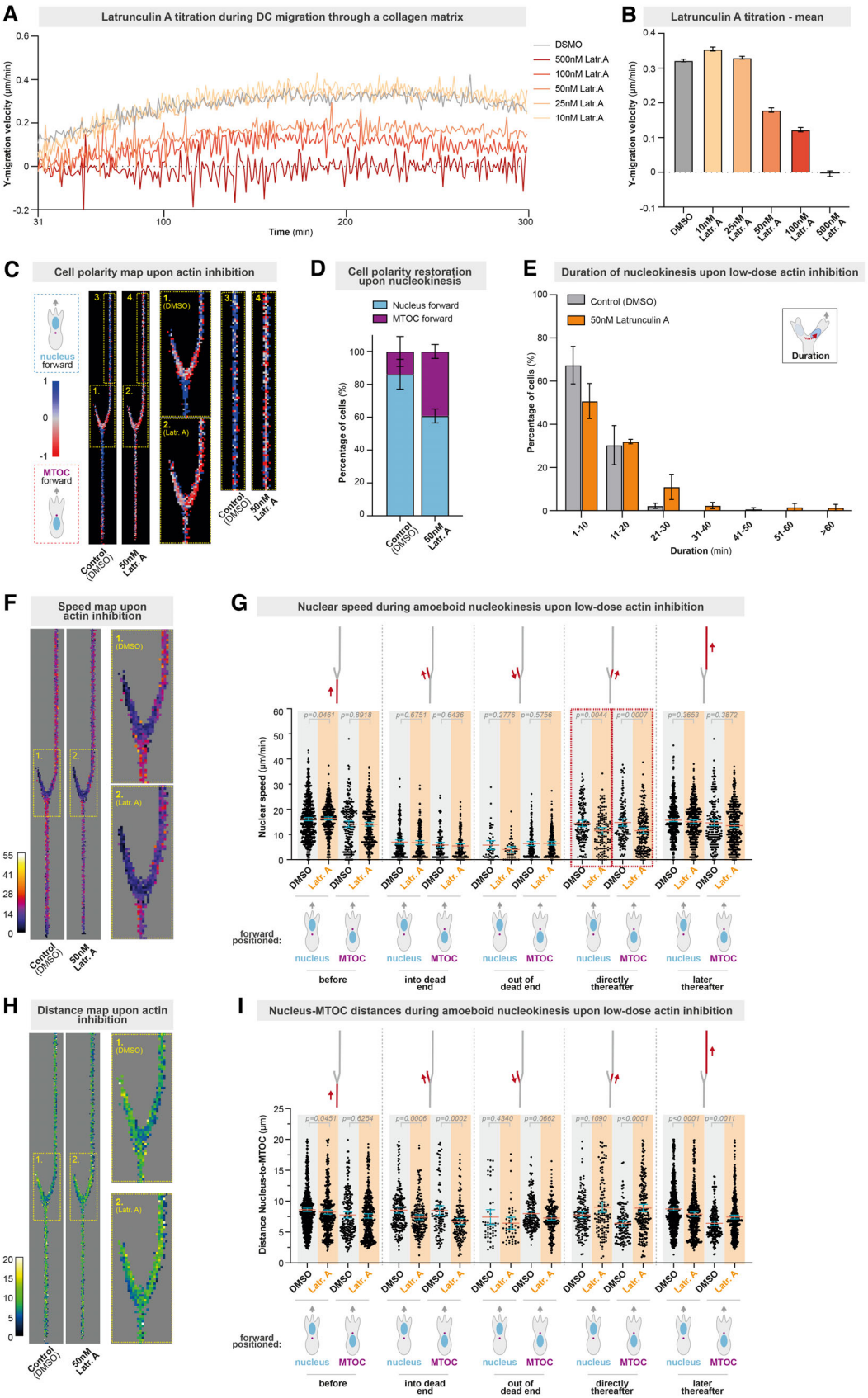

Figure EV5.